Syndecan-1 inhibits early stages of liver fibrogenesis by interfering with TGFβ1 action and upregulating MMP14

Eszter Regős[a], Hadeer Hesham Abdelfattah[a,b], Andrea Reszegi[a], László Szilák[c], Klára Werling[d], Gábor Szabó[e], András Kiss[f], Zsuzsa Schaff [f], Ilona Kovalszky[a], Kornélia Baghy[a,*]

[a]1st Department of Pathology and Experimental Cancer Research, Semmelweis University Budapest, Hungary
[b]Cairo University, Faculty of Science Zoology Department, Giza, Egypt
[c]Szilak Laboratories, Bioinformatics & Molecule-design Ltd. Szeged, Hungary
[d]2nd Department of Internal Medicine, Semmelweis University, Budapest, Hungary
[e]Institute of Experimental Medicine, Hungarian Academy of Science, Budapest, Hungary
[f]2nd Department of Pathology, Semmelweis University, Budapest, Hungary

[*]Corresponding author
Address: 1st Department of Pathology and Experimental Cancer Research, Semmelweis University, Üllői street 26, Budapest, Hungary, H1085
e mail: baghy.kornelia@med.semmelweis-univ.hu; bcory6@gmail.com
Telephone: +36 1 459 1500 ext 54449
Fax: +36 1 317 1074

Running title: Syndecan-1 in liver fibrogenesis

Highlights

- Transgenic mouse strain with hSDC1 overexpression in the liver was created.

- SDC1 overexpression exerted a protective effect in the first 2 month of fibrosis.

- Overexpressing SDC1 removes TGFβ1 and THBS1 from the liver by shedding.

- SDC1 promoted MMP14 synthesis/activity and the protease increased syndecan shedding.

- Loss of hSDC1 and heparan sulfate explains the suspension of protective effect.

Abstract

Increased expression of syndecan-1 is a characteristic feature of human liver cirrhosis. However, no data are available on the significance of this alteration. To address this question we designed a transgenic mouse strain that driven by albumin promoter, expresses human syndecan-1 in the hepatocytes. Liver cirrhosis was induced by thioacetamide in wild type and hSDC1$^{+/+}$ mice of the identical strain. The process of fibrogenesis, changes in signal transduction and proteoglycan expression were followed. In an *in vitro* experiment, the effect of syndecan-1 overexpression on the action of TGFβ1 was determined. Human syndecan-1 and TGFβ1 levels were measured by ELISA in the circulation. Without challenge, no morphological differences were observed between wild type and transgenic mice livers, although significant upregulation of phospho-Akt and FAK was observed in the latter. Fibrogenesis in the transgenic livers, characterized by picrosirius staining, collagen type I, and SMA levels, lagged behind that of control in the first and second months. Changes in signal transduction involved in the process of fibrogenesis, as SMAD, MAPK, Akt and GSK, pointed to the decreased effect of TGFβ1, and this was corroborated by the decreased mRNA expression of TIEG and the growth factor itself. *In vitro* experiments exposing the LX2 hepatic stellate cell line to conditioned media of wild type and syndecan-1 transfected Hep3B cell lines proved that medium with high syndecan-1 content inhibits TGFβ1-induced upregulation of SMA, TIEG, collagen type I and thrombospondin-1 expression. Detection of liver proteoglycans and heparan sulfate level revealed that their amounts are much higher in control transgenic liver, than that in the wild type. However, it decreases dramatically as a result of shedding after hepatic injury. Shedding is likely promoted by the upregulation of MMP14. As syndecan-1 can bind thrombospondin-1, and as our result demonstrated that the same is true for TGFβ1, shed syndecan-1 can remove the growth factor and its activator together into the systemic circulation. Taking together, our results indicate that the effect of syndecan-1 is accomplished on two levels: **a**, the shedded syndecan can bind, inhibit and remove TGFβ1; **b**, interferes with the activation of TGFβ1 by downregulation and binding thrombospondin-1, the activator of the growth factor. However, by the end of the fourth month the protective effect was lost, which is explained by the considerable decrease of syndecan-1 and the almost complete loss of heparan sulfate from the surface of hepatocytes.

Keywords: syndecan-1, liver fibrosis, TGFβ1, thrombospondin-1, heparan-sulfate, MMP14

Abbreviations: SDC1: syndecan-1; TGFβ1: transforming growth factor-β1; MAPK: matrix activated protein kinase; ECM: extracellular matrix; ERK: extracellular matrix regulated kinase; GSK: glycogen synthase kinase; αSMA: α smooth muscle actin; THBS1: thrombospondin-1; MMP: matrix metalloprotease; HCC: hepatocellular carcinoma; HS: heparan-sulfate; PG: proteoglycan. TA: thioacetamide; TIEG: TGFβ inducible early gene; TIMP: tissue inhibitor of metalloproteinases; PAI: plasminogen activator inhibitor; bFGF: basic fibroblast growth factor; PDGF: platelet-derived growth factor

1. Introduction

In spite of sustained progress in understanding various aspects of the disease, management of liver cirrhosis is still a major challenge in medicine. The etiology includes a series of diseases and conditions, including HBV, HCV, alcohol consumption, autoimmunity, or various metabolic diseases [1]. Although a few reports show complete regeneration of the liver after cirrhosis induced by HBV [2-4], except for liver transplantation, generally still lack appropriate therapeutic measures. During liver fibrosis, hepatic stellate cells and fibroblast of the portal triad are activated and differentiate into myofibroblasts, start to proliferate, and produce ECM proteins, as well as MMPs and MMP inhibitors (e.g. TIMPs and PAI-I) [5-7]. This process involves several other factors including macrophages and inflammatory cells. All of these secrete growth factors and cytokines creating a cascade of events, which result in the imbalance between connective tissue production and degradation [8, 9]. Among others, TGFβ1 and PDGF as well as bFGF are considered the most potent pro-fibrogenic cytokines in the liver [10].

Although syndecan-1 is recognized as an active player in wound healing [11], its role in liver fibrogenesis has not been characterized. Syndecan-1 (SDC1) is a transmembrane proteoglycan, member of the syndecan family. Its protein core carries three heparan sulfate and two chondroitin sulfate side chains covalently attached to the protein backbone. The molecule occupies a strategic position on the cell surface establishing interactions between the extracellular matrix and the cytoplasm. SDC1 binds the ECM and modulates the effect of various growth factors and their receptors. It is well documented that various proteases (e.g. MMPs) can cleave the ectodomain of SDC1 [12]. The released syndecan-1 functions as paracrine and autocrine modulator of signaling in the microenvironment [13, 14] and can be detected in the circulation [15]. SDC1 participates in various physiological and pathological

4

processes. In SDC1 overexpressing mice wound healing is delayed due to reduced cell proliferation induced by circulating syndecan-1 [16]. SDC1 overexpression protects against cardiac dysfunction, dilatation and myocardial infarction [17] and increased serum syndecan-1 levels are markers of heart failure with fibrosis [18]. The expression and serum concentration of the protein increases in liver diseases such as NAFLD [19], liver cirrhosis and HCC [20]. Released syndecan-1 is reported to be a useful marker in the diagnosis of liver fibrosis [15].

To better understand the role of syndecan-1 in hepatic diseases, the aim of this study was to characterize the role of syndecan-1 overexpression in the development of thioacetamide-induced liver cirrhosis.

2. Results

2.1. Hepatic fibrosis is attenuated in hSDC1^{+/+} mice

Morphometry of picrosirius stained slides showed equal amounts of connective tissue in untreated control and hSDC1^{+/+} livers. In the second month of TA exposure, the deposition of connective tissue in transgenic livers significantly lagged behind the control ones. However, by the end of the fourth month the values in the two groups leveled off, and the intensity of picrosirius staining in hSDC1 [+/+] became comparable to the control liver samples. (Fig. 1A,B).

2.2. Production and accumulation of collagen type I

On the immunostaining of untreated frozen liver specimens, reaction with collagen type I marks the blood vessels. In harmony with the picrosirius staining, TA exposure resulted in the accumulation of the protein in the acino-peripherial regions along the sinusoids. When compared to the control animals, the extent of collagen positivity until months four was lower in hSDC1^{+/+} livers where the two groups displayed similar intensity. Collagen was deposited in the fibrotic tissue forming pseudolobules. (Fig. 2A).

The expression of collagen type I mRNA steady-state level supported this result. In the first three months of TA treatment the type I collagen level was significantly higher in WT animals than in transgenic mice. However, its expression in the fourth month of fibrogenesis became almost equal in the two studied groups (Fig. 2B).

2.3. Activation of myofibroblasts

To detect the activated myofibroblasts, αSMA staining was carried out. In the control livers, SMA positivity confined to the smooth muscle cells of the blood vessels. The immunopositivity correlated with the localization of type I collagen at the end of the 4th month of TA exposure, indicating the presence of proliferating myofibroblasts. At that time point collagen and αSMA expression seemed to be balanced in wild type livers, whereas αSMA positivity was weaker and more localized than that of collagen type I in hSDC1$^{+/+}$ livers. This was supported by the Western blot as well, showing that αSMA intensity, seen in hSDC1$^{+/+}$ protein extracts, never exceeded the level observed wild type samples (Fig. 3).

2.4. Changes of MMPs in vivo.

Looking for the mechanisms implicated in the protracted development of liver fibrosis in hSDC1$^{+/+}$ mice the activity of MMP2 and MMP9 was determined. Although we could detect the active form of MMP2 on the zymograms, the activity between wild type and syndecan transgenic livers did not differ over the experimental period (data not shown). On the other hand MMP2 activation pointed toward MMP14 and certainly immunohistochemistry revealed elevated amount of reaction at time point TA2 in the hSCD1$^{+/+}$ livers (Fig. 4). Furthermore, in contrast with the other groups, the reaction was located not only to the nonparenchymal cells of the sinusoids, but it was present along the plasma membranes of hepatocytes. The enzyme expression dropped below the control level by the end of the fourth month.

2.5. Effect of syndecan-1 on the steady state levels of TGFβ1 and TIEG mRNA and the activation of Smad2 and Smad3 proteins

Without hepatic challenge hSDC1$^{+/+}$ livers contain less TGFβ1 mRNA than that of control livers. TA exposure upregulates the message both in the control and the hSCD1$^{+/+}$ livers. Although the upregulation in the transgenic livers is somewhat higher in the first two months, it declines by the end of the third month where the expression of the wild type samples reaches their maximal level. In the fourth month TGFβ1 expression drops to the control level, not showing any significant alteration (Fig. 5A).

TIEG mRNA expression of the wild type samples followed the expression pattern of TGFβ1. However, this was not the case in hSDC1$^{+/+}$ samples, where hardly any elevation of the mRNA could be detected. The difference between the TIEG expression of wild type and transgenic livers proved to be significant in control samples and at months two and four in TA-exposed groups (Fig. 5B).

In the untreated samples, the amount pSmad2 and pSmad3 levels were equal in both groups. At the second month of TA administration, the amount of both pSmads were significantly higher in the WT animals compared to that in the hSDC1$^{+/+}$ samples (Fig. 5C).

2.6. Modification of signal transduction by overexpression of human syndecan-1

Representative members of signaling pathways known to be implicated in the development of liver fibrosis were quantified to assess the effect of syndecan-1 overexpression on the development of TA-induced liver injury. In control hSDC1$^{+/+}$ livers, the expression levels of all proteins were higher than that in the wild types, reaching statistical significance at pAkt and FAK. Simultaneously, Erk1/2 and pAKT S473 from the first month of TA injury, NFκB, pAKT T308, pGSK3 from the second, and FAK from the 3rd month of TA injury increased more in the wild type than in the syndecan transgenic livers, suggesting an inhibitory role of the proteoglycan. In general, the differences could no longer be observed by the end of the fourth month of hepatic injury (Fig. 6).

2.7. Overexpression of syndecan-1 inhibits the action of TGFβ1

To address whether syndecan-1 interferes with TGFβ1 action, conditioned media of Hep3B hepatocellular carcinoma cell line that does not expresses syndecan-1 and syndecan-1 transfected Hep3B cells (HEP3B/SDC1) were co-cultured with LX2 immortalized Ito cells and treated with 2 ng/mL TGFβ1 for 48 h. Subsequently the expression levels of SMA and TIEG were measured. Co-cultures containing the medium of hSDC1 transfectant cells (HEP3B/SDC1/LX2) expressed significantly lower amounts of αSMA and TIEG mRNA compared to the wild type co-culture (HEP3B/LX2) (Fig.7A,B).

We characterized the production of collagen type I of LX2 cells growing in the media of the two hepatoma cell lines by using dot-blot. After TGFβ1 treatment, the level of type I collagen increased in the culture medium of both co-cultures, but in a less extent in that growing in HEP3B/SDC1 conditioned medium (Fig. 7C).

We also asked the question if the released syndecan-1 is capable to bind TGFβ1. To this end, immobilized human TGFβ1 was incubated with the culture medium of human syndecan-1 transfected hepatoma cells. After subsequent washing steps the anti-syndecan-1 antibody identified positive syndecan-1 reaction in the localization of TGFβ1 indicating the interaction between TGFβ1 and the shed syndecan-1 (Fig. 7D).

One of the major activator of latent TGFβ1 is thrombospondin-1 (THBS1). The amount of THBS1 increased after TGFβ1 exposure in case of medium HEP3B/LX2 co-

culture compared to untreated samples. On contrary, Hep3B/SDC1 medium/LX2 co-culture failed to produce excess amounts of THBS1 upon TGFβ1 treatment (Fig. 7E). To avoid the interference with the hepatoma cells, we repeated this experiment by cultivating LX2 cells only in the conditioned media of the two hepatoma cell lines. In this setup, hSDC1-containing medium inhibited the THBS1 production of both the control and TGFβ1 exposed LX2 cells. In this case, the TGFβ inhibitory effect was not complete indicating the role of cell-cell contact between LX2 and Hep3B/SDC1 cells, as well (Fig. 7F).

To prove that hSDC1 is capable to upregulate MMP14, caseinase activity of culture media from HEP3B/LX2 and HEP3B/SDC1/LX2 cocultures have been determined. As Fig.7G shows MMP14 is present in both media, however in a much lower extent in that of HEP3B/LX2, furthermore it seems to be mainly in inactive form, whereas both active and inactive enzyme is present in HEP3B/SDC1/LX2 sample. The enzyme activities do not respond to TGFβ1 exposure (Fig.7G).

2.8. Changes in human syndecan-1 and heparan sulfate expression after TA injury, and the concentration of human syndecan-1 and TGFβ1 in the circulation

When performing immunostaining, the antibody recognizing the extracellular domain of human syndecan-1 did not react with the mouse liver tissue (Fig. 8A). Control hSDC1$^{+/+}$ livers showed positive reaction along the sinusoids corresponding to the apico-basal surface of hepatocytes. Liver fibrosis enhanced the amount of hSDC1 at TA2 time point, but at the end of the experiments, we witnessed considerable loss of the proteoglycan. These results were confirmed by Western blot analyses as well (Fig. S2). Changes in heparan sulfate expression partially followed those of syndecan-1 (Fig. 8B). Progressive decrease occurred already from the 2nd month, until the end of the experiment. Changes in HS expression was different in wild type animals, where we observed upregulation at month 2, but the final outcome was complete loss (Fig. 8 A,B). Parallel with the decrease of hSDC1 and HS in the transgenic livers, concentration of shedded human syndecan-1 increased significantly in the circulation (Fig.8C). Although it did not reach the level of significance, concentration of TGFβ1 in the circulation of transgenic animals surpassed that of the controls at each time point (Fig.8D).

As seen on Western blots, mouse syndecan-1 expression is low in the control livers of wild type animals and progressively increases over time (Fig. S2). Compared to the wild type,

in hSDC1$^{+/+}$ livers mouse syndecan-1 expression is lower throughout the experimental period, presumably as a compensatory effect (Fig. S2).

3. Discussion

Following recent introduction of drugs capable to eradicate HCV, one of the major etiological factors responsible for development of liver cirrhosis, the next biomedical challenge is to reverse the fibrotic remodeling of the liver [21]. In general, the mode of action of the players implicated in fibrogenesis are well known [3]. However, current reports lack a detailed evaluation of the role of syndecan-1, the major cell surface proteoglycan of the healthy organ. This proteoglycan is upregulated in human liver cirrhosis, and its increased shedding and elevated serum concentration is a typical feature of liver fibrosis [15, 22]. Moreover, syndecan-1 appears to be required for proper wound healing. As liver cirrhosis has close relationship with wound healing and scar formation, it is likely that the overexpression of syndecan-1 in cirrhotic liver has clinical significance [23]. Its structure and localization places syndecan-1 into a central position in the events taking place in course of fibrogenesis. The current studies were designed to investigate whether syndecan-1 exerts protective effects against liver injury and fibrosis.

Transgenic mice expressing syndecan-1 in their liver did not show any particular phenotype without hepatic challenge. When animals were exposed to TA, syndecan-1 overexpression provided protection against liver fibrosis in the first two months. However, this protection ended by the fourth month of TA exposure, when picrosirius staining revealed equal intensity of connective tissue deposition in wild type and in hSDC1$^{+/+}$ livers.

As the accumulation of the connective tissue in an organ is a consequence of the imbalance in production and degradation, we attempted to characterize the events implicated in our liver fibrosis model, and study them in context with the actual expression or release of syndecan-1. The lower steady state levels of collagen type I mRNA, with the lower amount of αSMA on Western blot, and their decreased immunopositivity in hSDC1$^{+/+}$ livers in the first 3 months of TA injury supported the results of picrosirius staining, and indicated the protracted activation of fibrogenic (hepatic stellate cells and fibroblast) nonparenchymal liver cells. In addition, lower expression of TIEG mRNA, a validated indicator of TGFβ1 action, pointed to the decreased effect of the growth factor. The *in vivo* observed effect of syndecan-1 overexpression on TIEG mRNA level was confirmed *in vitro*, as well.

We clearly observed a difference in the mRNA level of TGFβ1 in hSDC1^{+/+} livers, which was somewhat higher at the first two months of TA injury and dropped after that, and legged behind the relative expression of the wild type livers. As TGFβ1 is capable to stimulate its own transcription, decrease in its mRNA steady state level can also be the consequence of its decreased availability [24]. Because overexpression of syndecan-1 is capable to decrease both TGFβ1 and TGFβ1 receptor expression [25] and heparan sulfate can negatively regulate TGFβ1 responsiveness [26], it is likely that these processes can delay fibrogenesis. Furthermore, our results highlighted another process that can be responsible for the clearance of the growth factor, namely the shedding of syndecan-1. We observed a progressive increase in the extracellular domain of syndecan-1 in the sera of transgenic animals throughout the entire experiment (Fig.7C). Parallel with this change the amounts of intrahepatic proteoglycans and heparan sulfate decreased, creating an inbalance between the liver and the circulation. The decrease was much more pronounced in hSDC1^{+/+} livers especially at the second month of TA injury. According to earlier reports, TGFβ1 binds heparan sulfates [27, 28] and the transmembrane proteoglycan syndecan-1 contains heparan sulfate side chains [29]. We managed to verify here that released syndecan-1 binds TGFβ1 and subsequently promotes the clearance of the growth factor into the circulation decreasing its local concentration. Although the changes did not prove significant, TGFβ1 ELISA of the serum supported our hypothesis.

Overexpression of syndecan-1 and the gradually increasing shedding with the resulting removal of TGFβ1 had profound impact on the SMAD, MAPK, Akt and Wnt pathways, all participating in fibrogenesis activation [30-34]. Whereas their expression at time point zero were equal or higher in SDC1^{+/+} livers, their expression started to decrease later on. Compared to fibrogenesis in wild type livers, the ERK1/2 pathway (itself can be activated by TGFβ1 [35]) became inhibited. This process was followed by decreased Akt phosphorylation and decreased inactivation of GSK3α. Akt phosphorylation at Ser[473] by MTORC2 complex is similarly regulated by TGFβ1 [36].

The HS binding matricellular protein thrombospondin-1 (THBS1) is one of the major activators of latent TGFβ1 [37-40]. It is synthesized mainly by the nonparenchymal liver cells. Considering its well-characterized activity in fibrogenesis, we hypothesized that it can play a role in our model. Indeed, we found decreased amounts of THBS1 in the syndecan-1 expressing hepatoma-LX2 cell co-culture system.

All of these findings indicate that syndecan-1 attenuates the development of liver fibrosis partly by binding and eliminating TGFβ1, partly by hindering its activation, presumably by interfering with the action of THBS1.

The dynamism of hSDC1 and MMP14 expression showed that at TA2 time point both are overexpressed in the transgenic liver, whereas no difference were detected in the expression of MMP2 and MMP9 over the experimental period. This correlation raised the possibility that syndecan-1 is capable to upregulate MMP14, which was proved by our in vitro experiments. Here we detected the protease in the culture medium, but the shedding of MMP14 is already published [41]. In contrast to MMP2 and MMP9, in our system its upregulation did not require the effect of TGFβ1. As it is published [42], we propose, that MMP14, upregulated by hSDC1, is responsible for the shedding of the proteoglycan. However, this mechanism initiates a vicious circle, as the more MMP14 is activated, the more hSCD1 is removed from the surface of hepatocytes, what we witnessed by the end of the experiment. This way, no syndecan-1 remains in the liver to bind and remove TGFβ1 and THBS1, and activate MMP14. In addition, decrease of HS content of the liver raises the possibility that heparanase is also implicated in this process, which is a further task to prove.

The role of MMP14 in the resolution of liver fibrosis by activation of MMP2 has been already published [43, 44]. Needless to say that in case of cessation of toxic injury the mechanism, proposed by our model is beneficial, and can help to reverse liver fibrosis, whereas it is insufficient at a prolonged toxic exposure.

4. Experimental Procedures

4.1. Generation of Syndecan-1 transgenic mice

To generate a mouse strain that overexpresses human syndecan-1 in their liver, we designed a vector containing the human syndecan-1 cDNA sequence driven by a mouse albumin promoter (Fig. S1A). A 3.6 kb DNA fragment was isolated from mAlb/hSynd1 plasmid with *Sal*I-*Eci*I digestion and subsequent electroelution. Fragments were purified and microinjected into inseminated FVB/N mouse oocytes and the oocytes were transferred into CD1 host females. The progenies were tested for the presence of the targeted gene. The isolated DNA was digested with EcoRI enzyme, which split an approximately 2,2 kb fragment with the HindIII sequence used as probe. The final product was detected on a 1% TBE agarose gel (Fig. S1B). The forward (f) and reverse (r) primers were as follows (f:

GGCTGTAGTCCTGCCAGAAG) and (r: GTATTCTCCCCCGAGGTTTC). After genotyping the transgene was found in one male and two females. Transgenic animals were backcrossed into the FVB/N background for nine generations until homozygosity. Animals were produced in the Institute of Experimental Medicine of the Hungarian Academy of Sciences. The expression level of human syndecan-1 was analyzed by fluorescence immunohistochemistry (Fig. S1C).

4.2. Induction of liver cirrhosis

For induction of liver cirrhosis, 30 wild type and 30 hSDC1$^{+/+}$ transgenic mice were exposed to thioacetamide (TA) dissolved in their drinking water (300 mg/L) from 1 month of age for 4 months. Six mice were sacrificed at each time-point at monthly intervals. Age-matched untreated animals with identical genetic background served as controls. At each time-point, body weight and the liver weight were recorded, and blood was collected. Half of the liver samples were frozen for further processing and the other half were fixed in 10% formaldehyde and embedded in paraffin for histological analysis. Paraffin sections were dewaxed in xylene and stained with hematoxylin- eosin and picrosirius red (PS). Stained sections were used for histological diagnosis. All animal experiments were conducted according to the ethical standards of the Animal Health Care and Control Institute, Csongrad County, Hungary (permit no. XVI/03047-2/2008).

4.3. Cell lines

LX2 human hepatic stellate (a kind gift from Dr. Scott Friedman) and Hep3B hepatocellular carcinoma cell lines (purchased from the ECACC (European Collection of Cell Cultures)) were cultured in DMEM-1000 (Dulbecco's Eagle Medium, Sigma Aldrich, St Louise, MO, USA) supplemented with 10% fetal bovine serum albumin (FBS, Sigma Aldrich) and 1% penicillin-streptomycin solution (Sigma Aldrich).

Transfection of Hep3B cell line was carried out with a syndecan-1-EGFP construct using Effectene reagent (Qiagen, Valencia, CA, USA) according to the manufacturer's instructions. Briefly, Hep3B cells were grown until 60% confluence and treated with 0.2 µg/mL EGFP syndecan expression vector, containing the full length cDNA of syndecan-1. The construction of the syndecan-1 plasmid is described elsewhere [45]. Co-cultivating of 1x10^5 LX2 and 5x10^4 Hep3B wild type, or syndecan-1 transfected Hep3B cells were carried out in a 6-well plate. The serum concentration of co-cultures was decreased to 0.5% for 12 h

and the cells were exposed to recombinant human TGFβ1 (Sigma Aldrich, Cat. No. T7039-2UG) at 2 ng/mL concentration for 48 hours [46].

The interaction between shedded syndecan-1 and LX-2 cell line was tested in an indirect cell culture model. Briefly, the culture media of Hep3B and syndecan-1 overexpressing Hep3B cells were harvested. The media were centrifuged to remove cell debris, and the supernatants were diluted in 1:1 ratio with DMEM-1000. The diluted media were applied only on LX2 cells, and TGFβ was administered as described above.

4.4. Morphometrical analysis

To determine the connective tissue content of liver samples, picrosirius red stained sections were analyzed with an Olympus microscope using a Cue-2 software (Olympus, Tokyo, Japan). At least five representative areas at a 10X magnification were considered from each section.

4.5. Immunostaining

Frozen sections of the liver were fixed in ice-cold methanol and washed with phosphate-buffered saline (PBS). Next, sections were blocked with 5% (w/v) bovine serum albumin (BSA, Sigma Aldrich) dissolved in PBS for 1 h. The slides were washed and incubated with primary antibodies in 1% (w/v) BSA/PBS overnight at 4°C. After washing, appropriate fluorescent secondary antibodies (Table 1) were applied for 60 min in dark. Nuclei were stained with DAPI (4',6'-diamidino-2-phenylindole). Pictures were taken with Nikon Eclipse E600 (Nikon, Tokyo, Japan) with the help of Lucia Cytogenetics software (Laboratory Imaging, Praha, Czech Republic). Details of antibodies used are found in Supplementary Table 1.

Formalin-fixed paraffin-embedded sections were solubilized in xylene and ethanol, then washed with distilled H_2O for 5 min. Antigen retrieval was performed in a pressure cooker using TRIS-EDTA buffer (10 mM TRIS, 1 mM EDTA, 0.05% Tween 20, pH=9) for 20 min. After cooling, slides were washed 3 times in PBS with 0.05% Tween20 (PBST). Next, endogenous peroxidase was inactivated by addition of 10% H_2O_2 dissolved in methanol for 10 min. After washing with PBST, 5 w/v% bovine serum albumin (BSA)/PBS containing 10% normal serum was applied for 1 h to prevent any nonspecific binding. Primary antibodies were applied overnight at 4°C. The next day, slides were washed 3 times in PBST, and then incubated with appropriate secondary antibodies conjugated either with horse reddish peroxidase or with biotin for 1 hour. A detailed list of primary and secondary antibodies and

their appropriate dilutions is provided in Supplementary Table 1. In case of human syndecan-1 primary antibody the slides were incubated for 1 h with rabbit anti-goat HRP antibody at RT. For MMP-14 antibody Novolink Polymer Detection kit (RE7150-K, Leica Biosystem, Wetzlar, Germany) and for heparan-sulfate antibody M.O.M. ImmPRESS HRP Polymer Kit (Vector Laboratories, Burlingame, CA) was used according to the manufacturer's protocol. Images were taken using Pannoramic 250 digital scanner (3DHistech Ltd., Budapest, Hungary).

4.6. Real-time RT-PCR

Total RNAs were isolated from the frozen livers, as well as the harvested cells for gene expression analyses. After homogenization, total RNA was isolated with Trizol reagent following the protocol provided by the manufacturer. The concentration and purity of the isolated RNAs were characterized by using an ND-1000 spectrophotometer. One µg total RNA was reverse-transcribed using the M-MLV Reverse Transciptase kit in the animal model and High-Capacity cDNA Reverse Transciptase Kit with RNase Inhibitor in the tissue culture experiment. Real time PCR was performed in a Step One Plus Real-Time PCR System using the ABI TaqMan Gene Expressions Assays (Supplementary Table 2.) for mice liver samples and PrimeTime qPCR Assays (Supplementary Table 2.) for cell samples. 18S RNA and GAPDH were used as controls. Samples were run in triplicate with 20 ng cDNA, using TaqMan Universal PCR MasterMix in 20 µL reaction volume. Reaction conditions were as follows: initial denaturing 95°C for 10 min followed by 40 cycles of denaturation at 95°C for 15 sec and annealing at 60°C for 1 min. The results were obtained as threshold cycle values, and the expression levels were calculated with the $2^{-\Delta\Delta Ct}$ equation. All reagents were purchased from Thermo-Fisher Scientific (Carlsbad, CA, USA), except for ND-1000 spectrophotometer (NanoDrop Technologies, Wilmington, DE, USA) and PrimeTime qPCR Assays (Integrated DNA Technologies, San Jose, CA, USA,)

4.7. Syndecan-1 and TGFβ1 ELISA

Collected blood samples were centrifuged for 10 min at 2400 rpm, and the plasma samples were transferred to a clean 1.5 mL tube. The amount of human syndecan-1 was quantified in the plasma using the CD138 ELISA Kit (Diaclone, Gen Probe, Besançone, France, Cat. No. 850.640.096) The plasma level of mouse TGFβ1 was measured using the mouse TGFβ1 ELISA Kit (R&D System Minneapolis, MN, USA) according to the

manufacturer's protocol. The color reaction was detected at 450 nm with a Multiskan MS ELISA Reader (A.A. LabSystem, Ramat-Gan, Israel).

4.8. Western Blot and Dot Blot Analysis

Frozen liver samples and cells were lysed in a buffer containing 20 mM Tris-HCl pH 7.5, 150 mM NaCl, 2 mM EDTA, 1 mM PMSF, 10 mM sodium orthovanadate, 10 mM NaF, 1:200 Protease Inhibitor Cocktail (P8340, Sigma Aldrich), and 0.5 % Triton X-100. Protein concentrations were measured as described before by Bradford [47]. Fifteen µg of total proteins were mixed with loading buffer containing β-mercaptoethanol and were incubated at 95 C for 5 min. Denatured samples were loaded onto a 10% polyacrylamide gel and run for 30 min at 200 V on a Mini Protean vertical electrophoresis equipment (Bio-Rad, Hercules, CA). Proteins were transferred onto a PVDF membrane (Merck Millipore. Billerica, MA) by blotting for 1.5 h at 100 V. For dot blot analysis, 200 µL of cell medium was applied onto PVDF membrane. Ponceau staining was applied to determine blotting efficiency in both Western and Dot blot analysis. Membranes were blocked with 5 w/v% non-fat dry milk (Bio-Rad) or bovine serum albumin (BSA) for phosphorylated proteins in TBS for 1 h followed by incubation with the primary antibodies at 4 °C for 16 overnight. Membranes were washed 3 times with TBS containing 0.5 v/v% Tween-20, then were incubated with appropriate HRP-conjugated secondary antibodies for 1 h. Immunodetection was performed by peroxidase reaction or ECL (Pierce, Rockford, IL, USA). A detailed list of the antibodies used in this study is presented in Supplementary Table 1.

4.9. Syndecan-1 and TGFβ1 interaction

In order to detect the interactions between released syndecan-1 and TGFβ1, serially diluted growth factor (Sigma Aldrich) was applied onto a PVDF membrane. Next, the membranes were blocked with 5% non-fat dry milk dissolved in TBS and incubated with the culture media of syndecan-1 transfected Hep3B cells overnight at 4°C. Dot blot of 50 µL medium of syndecan-1 transfected Hep3B cells were used as positive control. Next, the membranes were washed with TBS and probed with an anti-syndecan-1 antibody that recognize the extracellular domain of human syndecan-1 (EPR6454, Merck) in 1:500 dilution for 16 h at 4°C. After washing, the membranes were incubated with a HRP- conjugated secondary antibody (Supplementary Table 1.) for 1 h at room temperature. Images were visualized with Super Signal West Pico Chemiluminescent Substrate Kit and recorded by

using a Kodak Image Station 4000 MM Digital Imaging System (Kodak, Rochester, NY, USA).

4.10. Proteoglycan isolation

In order to determine the amount of proteoglycans (PGs) and heparan sulfate on Western-blot total PG was isolated from frozen liver samples after homogenization in liquid nitrogen. The extraction buffer added to liver samples contained 4 M Guanidium-HCl, 50 mM Sodium-acetate, 5 mM NEM, 0.5 mM PMSF, 0.001 w/v % soy-bean tripsin inhibitor (Sigma Aldrich) and 5000 U/ml aprotinin (Richter Gedeon, Budapest, Hungary). The samples were incubated for 20h at 4°C, pH=5.0. After centrifugation, trichloroacetic acid (TCA) was added to the supernatants reaching a final concentration of 10 v/v%. Precipitated material was removed by centrifugation at 11 000 RPM for 30 min. The supernatants neutralized were loaded into cellulose dialysis membrane tubes (D9277, Sigma Aldrich) and were dialyzed against buffer containing 7M urea 0.05 M Tris-HCl, 5mM NEM, 5mM PMSF, 0.0001 w/v% soy-bean tripsin inhibitor (Sigma Aldrich) and 5000 U/ml aprotinin, pH=7.0 (Richter Gedeon, Budapest, Hungary). For anion exchange chromatography DE52 diethylaminoethyl cellulose (Whatman) columns were used equilibrated with 7 M Urea and 50 mM NaCl, pH=7.0. The columns were washed with buffers with increasing sodium concentration and proteoglycans were eluted with 7 M Urea and 0.8 M NaCl at pH=7. The eluted samples were precipitated with absolute ethanol in a ratio of 1:9 overnight at -70°C. The samples were loaded on to Mini-Protean TGX Precast 4-20% Gradient Gel (BioRad). The electrophoresis was performed as previously described at the Western-blot analysis section. The gels were stained in 5% Alcian-Blue in 2% acetic-acid then destained in 7% acetic acid.

4.11. GAG isolation

Equal volume of frozen liver samples were lysed in 10 ml 0.1 M Tris-HCl (pH=7.9), and diluted with 4X volume of acetone, incubated overnight at room temperature. After centrifugation at 3000 RPM for 30 min at 4°C, the supernatant was removed and the pellet was washed with acetone three times. The pellets were air dried and then were resuspended in 5 ml 0.1 M Tris-HCl (pH=7.9). Non-specific protease (Cat.No. P8811, Sigma Aldrich) was added to degrade proteins in the samples and were incubated for three days at 50°C. For β-elimination, NaOH was applied in a final concentration of 0.5 M and incubated for 4 hours at RT. After incubation the pH of the samples were reduced to 7.5 with HCl. To elliminate the

residual macromolecules from the samples trichloroacetic acid was used at 10 v/v% final concentration for 4°C on ice for 1 hour. After centrifugation at 3000 RPM for 30 min at RT the supernatants were loaded into cellulose dialysis membrane tubes (Cat. No. D9527, Sigma Aldrich), and were dialyzed against dH_2O. After dialysis, the samples were precipitated with cetylpyridinum-chloride (CPC, Cat. No.: C9002, Sigma Aldrich) and Na_2SO_4 at the final concentration of 0.5% and 0.02M respectively. After centrifugation at 5000 RPM for 1 hour at 4°C 1 ml of 2 M NaCl and 96% ethanol in a 100:15 dilution ratio was added to the samples and incubated for 5 min at RT to unfold the GAG-CPC complex. The samples were precipitated at 4°C for 24 hour with 4X volume of 96% ethanol containing 1 w/v% sodium acetate and 1 v/v% acetic acid. After centrifugation, the pellets were washed with acetone, air-dried and resuspended in dH_2O. The amount of GAG was determined by dimethylmethylene blue assay [48]. The absorbance was measured at 525 nm wavelength.

4.12. Caseinase assay

For caseinase assay 20 µl of cell culture media was used and 5% FBS (Foetal Bovine Serum, Cat. No. F0804, Sigma Aldrich) was applied as positive control. Briefly, aliquots of each sample were analyzed on a 7.5% SDS-polyacrylamide gel, containing 3 µg/ml casein (α-Casein from bovine milk, C6780, Sigma Aldrich), 5 µl/ml fibronectin (Cat. No. F1141, Sigma Aldrich) and 10 µl/ml Matrigel (Cat. No. E1270, ECM Gel from Engelbreth-Holm-Swatm murine sarcoma, Sigma Aldrich). After electrophoresis at 200 V for 35 min, the gel was washed in 2.5% Triton X-100 for 30 min, then incubated for 20 hours at 37°C in a solution containing 50 mM Tris, pH=7.5, and 10 mM $CaCl_2$. Gels were fixed in 30% methanol and 10% acetic acid for 30 min at room temparature, then stained with Coomassie Brilliant Blue for another 30 min. Areas of enzyme activity appeared as transparent bands on the blue background.

4.13. Statistical analysis

All statistical analyses were made with GraphPad Prism 6.01 software (Graphpad Software Inc.). Datawere tested for normal distribution by D'Agostino and Pearson's omnibus normality test. Significance of changes were tested by non-parametric tests (Mann-Whitney) or Students' t-tests depending on the distribution of the data. Significance levels were selected as *:p<0.05; **:p<0.01; and ***:p<0.001.

5. Acknowledgement

6. References

[1] D. Schuppan, N.H. Afdhal, Liver cirrhosis, Lancet 371(9615) (2008) 838-51.

[2] A.J. van der Meer, M. Sonneveld, J.N. Schouten, H.L. Janssen, [Reversibility of hepatic fibrosis], Ned. Tijdschr. Geneeskd. 158 (2014) A6790.

[3] F. Saffioti, M. Pinzani, Development and Regression of Cirrhosis, Dig. Dis. 34(4) (2016) 374-81.

[4] T. Kisseleva, D.A. Brenner, Inactivation of myofibroblasts during regression of liver fibrosis, Cell Cycle 12(3) (2013) 381-2.

[5] G. Biagini, G. Ballardini, Liver fibrosis and extracellular matrix, J. Hepatol. 8(1) (1989) 115-24.

[6] A.M. Gressner, Liver fibrosis: perspectives in pathobiochemical research and clinical outlook, Eur. J. Clin. Chem. Clin. Biochem. 29(5) (1991) 293-311.

[7] A.M. Gressner, Hepatic fibrogenesis: the puzzle of interacting cells, fibrogenic cytokines, regulatory loops, and extracellular matrix molecules, Z. Gastroenterol. 30 Suppl 1 (1992) 5-16.

[8] S.L. Friedman, Mechanisms of hepatic fibrogenesis, Gastroenterology 134(6) (2008) 1655-69.

[9] S. Ueha, F.H. Shand, K. Matsushima, Cellular and molecular mechanisms of chronic inflammation-associated organ fibrosis, Front. Immunol. 3 (2012) 71.

[10] G.O. Elpek, Cellular and molecular mechanisms in the pathogenesis of liver fibrosis: An update, World J. Gastroenterol. 20(23) (2014) 7260-76.

[11] M.A. Stepp, S. Pal-Ghosh, G. Tadvalkar, A. Pajoohesh-Ganji, Syndecan-1 and Its Expanding List of Contacts, Adv Wound Care (New Rochelle) 4(4) (2015) 235-249.

[12] T. Manon-Jensen, Y. Itoh, J.R. Couchman, Proteoglycans in health and disease: the multiple roles of syndecan shedding, FEBS J. 277(19) (2010) 3876-89.

[13] S.E. Gill, S.T. Nadler, Q. Li, C.W. Frevert, P.W. Park, P. Chen, W.C. Parks, Shedding of Syndecan-1/CXCL1 Complexes by Matrix Metalloproteinase 7 Functions as an Epithelial Checkpoint of Neutrophil Activation, Am. J. Respir. Cell. Mol. Biol. 55(2) (2016) 243-51.

[14] V.C. Ramani, R.D. Sanderson, Chemotherapy stimulates syndecan-1 shedding: a potentially negative effect of treatment that may promote tumor relapse, Matrix Biol. 35 (2014) 215-22.

[15] I. Zvibel, P. Halfon, S. Fishman, G. Penaranda, M. Leshno, A.B. Or, Z. Halpern, R. Oren, Syndecan 1 (CD138) serum levels: a novel biomarker in predicting liver fibrosis stage in patients with hepatitis C, Liver Int. 29(2) (2009) 208-12.

[16] V. Elenius, M. Gotte, O. Reizes, K. Elenius, M. Bernfield, Inhibition by the soluble syndecan-1 ectodomains delays wound repair in mice overexpressing syndecan-1, J. Biol. Chem. 279(40) (2004) 41928-35.

[17] D. Vanhoutte, M.W. Schellings, M. Gotte, M. Swinnen, V. Herias, M.K. Wild, D. Vestweber, E. Chorianopoulos, V. Cortes, A. Rigotti, M.A. Stepp, F. Van de Werf, P. Carmeliet, Y.M. Pinto, S. Heymans, Increased expression of syndecan-1 protects against cardiac dilatation and dysfunction after myocardial infarction, Circulation 115(4) (2007) 475-82.

[18] J. Tromp, A. van der Pol, I.T. Klip, R.A. de Boer, T. Jaarsma, W.H. van Gilst, A.A. Voors, D.J. van Veldhuisen, P. van der Meer, Fibrosis marker syndecan-1 and outcome in patients with heart failure with reduced and preserved ejection fraction, Circ. Heart Fail. 7(3) (2014) 457-62.

[19] Y. Yilmaz, F. Eren, Y. Colak, E. Senates, C.A. Celikel, N. Imeryuz, Hepatic expression and serum levels of syndecan 1 (CD138) in patients with nonalcoholic fatty liver disease, Scand. J. Gastroenterol. 47(12) (2012) 1488-93.

[20] I. Kovalszky, J. Dudas, M. Gallai, P. Hollosi, P. Tatrai, E. Tatrai, Z. Schaff, [Proteoglycans in the liver], Magy. Onkol. 48(3) (2004) 207-13.

[21] Y.K. Jung, H.J. Yim, Reversal of liver cirrhosis: current evidence and expectations, Korean J. Intern. Med. 32(2) (2017) 213-228.

[22] P. Tatrai, K. Egedi, A. Somoracz, T.H. van Kuppevelt, G. Ten Dam, M. Lyon, J.A. Deakin, A. Kiss, Z. Schaff, I. Kovalszky, Quantitative and qualitative alterations of heparan sulfate in fibrogenic liver diseases and hepatocellular cancer, J. Histochem. Cytochem. 58(5) (2010) 429-41.

[23] V. Natarajan, E.N. Harris, S. Kidambi, SECs (Sinusoidal Endothelial Cells), Liver Microenvironment, and Fibrosis, Biomed Res. Int. 2017 (2017) 4097205.

[24] C.C. Bascom, J.R. Wolfshohl, R.J. Coffey, Jr., L. Madisen, N.R. Webb, A.R. Purchio, R. Derynck, H.L. Moses, Complex regulation of transforming growth factor beta 1, beta 2, and beta 3 mRNA expression in mouse fibroblasts and keratinocytes by transforming growth factors beta 1 and beta 2, Mol. Cell. Biol. 9(12) (1989) 5508-15.

[25] T. Szatmari, F. Mundt, G. Heidari-Hamedani, F. Zong, E. Ferolla, A. Alexeyenko, A. Hjerpe, K. Dobra, Novel genes and pathways modulated by syndecan-1: implications for the

proliferation and cell-cycle regulation of malignant mesothelioma cells, PLoS One 7(10) (2012) e48091.

[26] C.L. Chen, S.S. Huang, J.S. Huang, Cellular heparan sulfate negatively modulates transforming growth factor-beta1 (TGF-beta1) responsiveness in epithelial cells, J. Biol. Chem. 281(17) (2006) 11506-14.

[27] J. Lee, S. Wee, J. Gunaratne, R.J. Chua, R.A. Smith, L. Ling, D.G. Fernig, K. Swaminathan, V. Nurcombe, S.M. Cool, Structural determinants of heparin-transforming growth factor-beta1 interactions and their effects on signaling, Glycobiology 25(12) (2015) 1491-504.

[28] M. Lyon, G. Rushton, J.T. Gallagher, The interaction of the transforming growth factor-betas with heparin/heparan sulfate is isoform-specific, J. Biol. Chem. 272(29) (1997) 18000-6.

[29] R. Kokenyesi, M. Bernfield, Core protein structure and sequence determine the site and presence of heparan sulfate and chondroitin sulfate on syndecan-1, J. Biol. Chem. 269(16) (1994) 12304-9.

[30] P. Xu, Y. Zhang, Y. Liu, Q. Yuan, L. Song, M. Liu, Z. Liu, Y. Yang, J. Li, D. Li, G. Ren, Fibroblast growth factor 21 attenuates hepatic fibrogenesis through TGF-beta/smad2/3 and NF-kappaB signaling pathways, Toxicol. Appl. Pharmacol. 290 (2016) 43-53.

[31] H. Qiang, Y. Lin, X. Zhang, X. Zeng, J. Shi, Y.X. Chen, M.F. Yang, Z.G. Han, W.F. Xie, Differential expression genes analyzed by cDNA array in the regulation of rat hepatic fibrogenesis, Liver Int. 26(9) (2006) 1126-37.

[32] P. Sysa, J.J. Potter, X. Liu, E. Mezey, Transforming growth factor-beta1 up-regulation of human alpha(1)(I) collagen is mediated by Sp1 and Smad2 transacting factors, DNA Cell Biol. 28(9) (2009) 425-34.

[33] F. Xu, C. Liu, D. Zhou, L. Zhang, TGF-beta/SMAD Pathway and Its Regulation in Hepatic Fibrosis, J. Histochem. Cytochem. 64(3) (2016) 157-67.

[34] J. Voelkl, S. Mia, A. Meissner, M.S. Ahmed, M. Feger, B. Elvira, B. Walker, D.R. Alessi, I. Alesutan, F. Lang, PKB/SGK-resistant GSK-3 signaling following unilateral ureteral obstruction, Kidney Blood Press. Res. 38(1) (2013) 156-64.

[35] J.M. Carthy, A. Sundqvist, A. Heldin, H. van Dam, D. Kletsas, C.H. Heldin, A. Moustakas, Tamoxifen Inhibits TGF-beta-Mediated Activation of Myofibroblasts by Blocking Non-Smad Signaling Through ERK1/2, J. Cell. Physiol. 230(12) (2015) 3084-92.

[36] J. Li, J. Ren, X. Liu, L. Jiang, W. He, W. Yuan, J. Yang, C. Dai, Rictor/mTORC2 signaling mediates TGFbeta1-induced fibroblast activation and kidney fibrosis, Kidney Int. 88(3) (2015) 515-27.

[37] M.T. Sweetwyne, J.E. Murphy-Ullrich, Thrombospondin1 in tissue repair and fibrosis: TGF-beta-dependent and independent mechanisms, Matrix Biol. 31(3) (2012) 178-86.

[38] A. Sasaki, H. Naganuma, E. Satoh, T. Kawataki, K. Amagasaki, H. Nukui, Participation of thrombospondin-1 in the activation of latent transforming growth factor-beta in malignant glioma cells, Neurol. Med. Chir. (Tokyo) 41(5) (2001) 253-9.

[39] J.E. Murphy-Ullrich, M. Poczatek, Activation of latent TGF-beta by thrombospondin-1: mechanisms and physiology, Cytokine Growth Factor Rev. 11(1-2) (2000) 59-69.

[40] J.E. Murphy-Ullrich, M.J. Suto, Thrombospondin-1 regulation of latent TGF-beta activation: A therapeutic target for fibrotic disease, Matrix Biol. (2017).

[41] P. Osenkowski, M. Toth, R. Fridman, Processing, shedding, and endocytosis of membrane type 1-matrix metalloproteinase (MT1-MMP), J. Cell. Physiol. 200(1) (2004) 2-10.

[42] T. Manon-Jensen, H.A. Multhaupt, J.R. Couchman, Mapping of matrix metalloproteinase cleavage sites on syndecan-1 and syndecan-4 ectodomains, FEBS J. 280(10) (2013) 2320-31.

[43] M. Arthur, The role of matrix degradation in liver fibrosis, in: G.R. AM Gressner (Ed.), Molecular and cell biology of liver fibrogenesis, Kluwer Academic Publishers, Dordrecht, 1992, pp. 213-227.

[44] M. Roderfeld, Matrix metalloproteinase functions in hepatic injury and fibrosis, Matrix Biol. (2017).

[45] B. Peterfia, T. Fule, K. Baghy, K. Szabadkai, A. Fullar, K. Dobos, F. Zong, K. Dobra, P. Hollosi, A. Jeney, S. Paku, I. Kovalszky, Syndecan-1 enhances proliferation, migration and metastasis of HT-1080 cells in cooperation with syndecan-2, PLoS One 7(6) (2012) e39474.

[46] K. Baghy, K. Dezso, V. Laszlo, A. Fullar, B. Peterfia, S. Paku, P. Nagy, Z. Schaff, R.V. Iozzo, I. Kovalszky, Ablation of the decorin gene enhances experimental hepatic fibrosis and impairs hepatic healing in mice, Lab. Invest. 91(3) (2011) 439-51.

[47] M.M. Bradford, A rapid and sensitive method for the quantitation of microgram quantities of protein utilizing the principle of protein-dye binding, Anal. Biochem. 72 (1976) 248-54.

[48] V. Coulson-Thomas, T.F. Gesteria, Dimethylmethylene Blue Assay (DMMB), Bio-protocol 4(18) (2014) e1236.

7. Legend to Figures

Figure 1. Hepatic fibrosis is accentuated in hSDC1$^{+/+}$ animals. A: Picrosirius stained sections from the liver of wild type and hSDC1$^{+/+}$ animals without treatment (CTL), and in the second (TA2) and fourth (TA4) month of thioacetamide exposure. Scale bar: 150 μm. B: Morphometry of the picrosirius stained sections revealed protracted development of liver fibrosis in hSDC1$^{+/+}$ transgenic mice. Values represent the mean (%)±s.e.m. of six animals in each group. Significance level: *:p<0.05 **:p<0.01

Figure 2. Changes in collagen type I in hepatic fibrosis in hSDC1$^{+/+}$ mice. A: Collagen type-I immunostaining. On the control liver sections the reaction labels the blood vessels. The reaction labels the TA-induced liver fibrosis in the acino-periherial regions and along the sinusoids, which is well discernible in control livers at the 2nd month of TA exposure but modest in hSDC1$^{+/+}$ livers. Scale bar: 200 μm. The intensity of collagen immunoreaction became equal at TA4 time point. B: Relative expression of collagen-type I mRNA of hSDC1$^{+/+}$ livers compared to that of the wild type animals. Values represent the mean (%)±s.d. of six animals in each group. Significance level: *:p<0.05

Figure 3. Changes in α-smooth muscle actin (αSMA) in liver sections. A: αSMA immunostaining. In control samples the reaction was observed around the blood vessels. At TA2 and TA4 time points, when myofibroblasts appear in the fibrotic septa, the intensity of the reaction was weaker in hSDC1$^{+/+}$ livers. Scale bar 200 μm. B: αSMA Western-blot confirmed the results of immunohistochemistry, although no difference between the expression of wild type and hSDC1$^{+/+}$ livers was observed at the time point 3 month. Differences between TA1, TA2 and TA4 time points are significant with p values of <0.05 and <0.001 respectively. n=6, data are expressed as mean±s.d.

Figure 4. Immunohistochemistry of MMP14 in wild type and hSDC1$^{+/+}$ mice over the 4 months period. The intensity of MMP14 is similar in the control groups, where the immunoreaction is located to the sinusoidal area. At time point TA2 strong overexpression occurs in the hSDC1$^{+/+}$ livers, where the reaction aligns the sinusoids and can be detected on the plasma membranes of hepatocytes as well. At the end of the experiments, the expression drops below that of the control in both groups. Arrows point to the reaction on the plasmamembranes of the hepatocytes.

Figure 5. Analysis of TGFβ1 and related molecules. A: mRNA expression of TGFβ1. The steady state level of the growth factor mRNA is gradually increasing until the 2nd months of TA exposure. After that it increases further in the wild type liver, whereas it drops in the hSDC1^{+/+} livers below the values of wild type samples. B: starting from the 2nd month steady state level of TIEG increases in wild type liver, but its induction fails in transgenic livers. C: pSmad2 and pSmad3 Western-blots showing increased phosphorylation of the protein at 2nd months of TA exposure in the wild type livers. Values represent the mean (%)±s.d. of six animals in each group. Significance level: * p<0.05

Figure 6. Alterations in signal transduction pathways of the liver cells after TA exposure. pERK1/2 of wild type liver is activated already in the first month of TA exposure in wild type livers, reaching maximal intensity at TA2 time point but hardly any activation was observed in hSDC1^{+/+} livers. At TA1 and TA2 time points pAkt Ser 473 of hSDC1^{+/+} livers was higher than that of control, but decreased thereafter, together with the decreased activation of pGSK3αβ at TA2, TA3 and TA4 time points. NFκB showed similar tendency, at TA1-TA3 time points, but the expression became equal at TA4. The behavior of FAK l also followed the same tendency. Except pGSK3αβ, at TA4 time point the intensity of signaling pathways leveled off.

Figure 7. *In vitro* experiments showing the effect of syndecan-1 overexpression on LX2 cells. LX2 cells were co-cultivated either with syndecan-1 negative Hep3B or syndecan-1 transfected Hep3B/SDC cells. Subsequently, the cells were exposed to TGFβ1 and these cells were compared to the untreated, control groups. We determined mRNA levels of αSMA (A), TIEG (B), collagen type I protein upon TGFβ1 treatment (C), the binding of syndecan-1 to the immobilized TGFβ1 (D), and changes in thrombospondin-1 level (THBS1) (E). Stimulation of THBS1 of LX2 cells was repeated with the conditioned media of the 2 hepatoma cell lines to exclude the effect of the hepatoma cells (F). Detection of shed MMP14 in the medium produced by LX2-Hep3B cocultures (G). MMP14 production is much higher in the HEP3B/SDC1/LX2 cocultures.

In the presence of syndecan-1, SMA production decreases both in the control and in the TGFβ1 treated group. TIEG was inhibited only in TGFβ1 exposed samples, similarly to THBS1. The medium of HEP3B/SDC cells contained ample amounts of released syndecan-1, which interacted with the immobilized TGFβ1. No syndecan-1 was detectable in the medium

of HEP3B cells (D). HEP3B/SDC1 cells synthesize considerable amount of MMP14. Pictures are the representatives of four independent experiments. Data are expressed as mean±s.d.

Figure 8. Detection of human syndecan-1, heparan sulfate and plasma levels of hSDC1 and TGFβ1. Paraffin embedded control and TA exposed liver specimens at time point TA2 and TA4 were reacted with polyclonal anti human SDC1 antibody recognizing the extracellular domain of the proteoglycan. The antibody did not react with the mouse liver, whereas positive reaction was obtained in transgenic livers. Here the intensity of staining increased at time point TA2 but considerable decrease was observed at time point TA4 (A). Immunoreaction of hSDC1$^{+/+}$ livers with the monoclonal anti-heparan sulfate antibody, clone 10E4 was the most intensive, but it decreased gradually by the end of the experiments. In case of wild type animals the peak of HS expression was seen at TA2 time point and the reaction vanished by the end of the 4th month. (B) Plasma levels of syndecan-1 (C) and TGFβ1 (D). Parallel with the loss of HS in the livers, the circulating human syndecan-1 concentration increases, and there is more circulating TGFβ1 in the circulation of transgenic animals. n=6, data are expressed as mean±s.d.

Figure 9. Molecular mechanisms participating in the protective effect of syndecan-1 overexpression.
Heparan sulfate chains of syndecan-1 can bind both TGFβ1 and thrombospondin-1 (THBS1). This action inhibits the activation of the latent growth factor. Thus, the availability of active TGFβ1 decreases. Furthermore, hSDC1 overexpression upregulates MMP14, resulting in increased shedding of syndecan-1. Shed syndecan-1 enters into the circulation together with TGFβ1 cargo and presumably also with THBS1. Decreased activation and availability of TGFβ1 downregulates signaling, implicated in the enhanced synthesis of molecules needed to fibrogenesis.

Supplementary Figure S1
Cloning strategy and characterization of hSDC$^{+/+}$ mice. Syndecan-1 is driven by the albumin promoter, thus the protein expresses only in the hepatocytes. (A) A 3.6 kb DNA containing the promoter and the cDNA of syndecan-1 was cut out, cleaned and microinjected into FVB/N mouse oocytes. With genotyping the transgene was found in one male and two females. The transgenic animals were backcrossed into the FVB/N background for nine

generations until homozygosity (B). Immunoreaction with monoclonal anti-human syndecan-1 antibody (C) that recognizes the extracellular domain of the molecule.

Supplementary Figure S2. Western blots of proteoglycans isolated from the mouse livers. The upper panel shows the immunoreaction of mouse syndecan-1, the lower panel is blotted with human syndecan-1. Mouse syndecan-1 expression is low in the control livers of wild type animals and progressive increases over time. Presumably as a compensatory effect its expression is always lower in the control, TA2 and T4 hSDC1$^{+/+}$ livers. Antibody, against the intracellular domain of human syndecan detected positive reaction on case of control liver, which in harmony with the immunohistochemistry increased at TA2 and decreased at TA4 time points. Modest cross reactions were fonund in the samples of wild type animals, which were not seen on immunohistochemistry.

Measurement of the GAG concentrations, isolated from the livers showed higher amount of total GAG in hSDCN1 transgenic livers, which dropped and leveled by the end of the second month most probably because of increased shedding. Considering the severe decrease of HS in the livers at month 4, the increased GAG content rather corresponds the DS, and CS chains of the deposited extracellular matrix.

Figure 1.
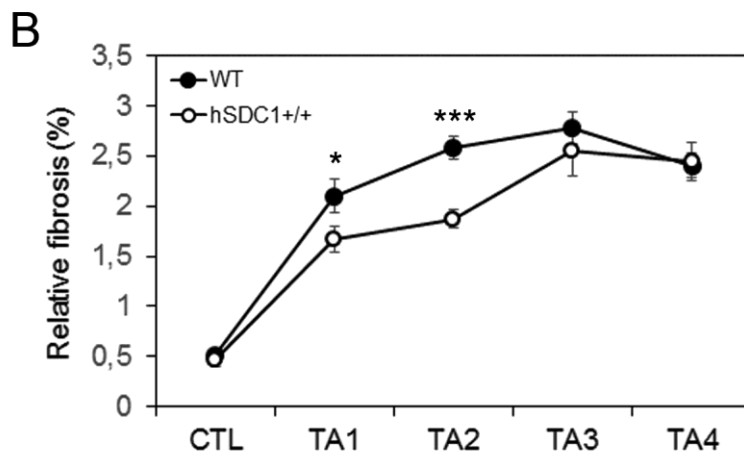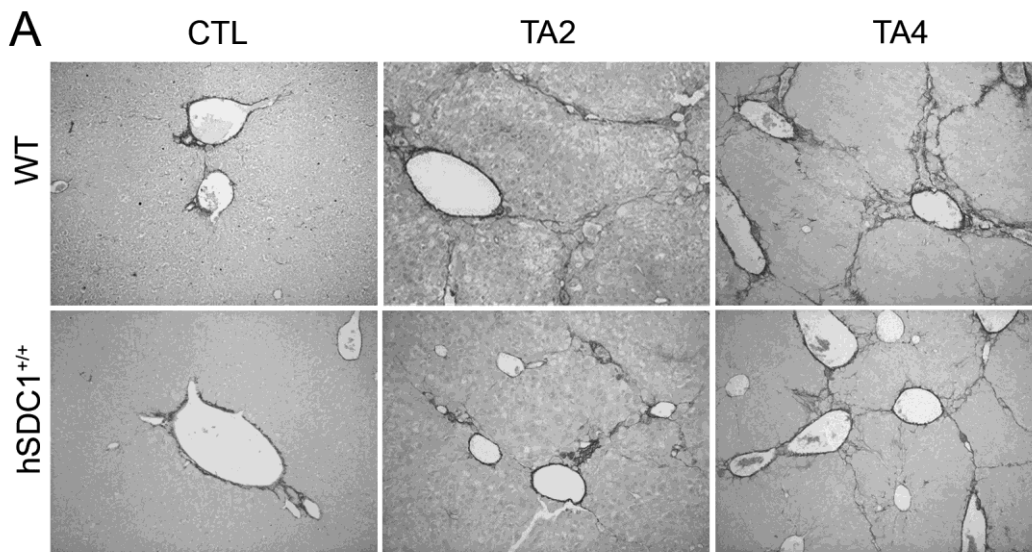
Figure 2.
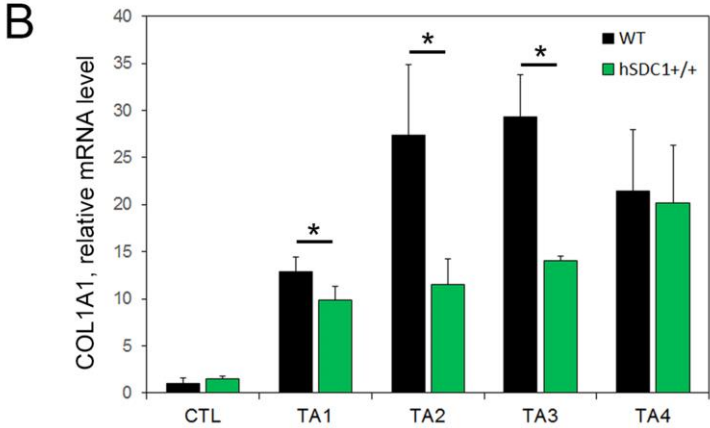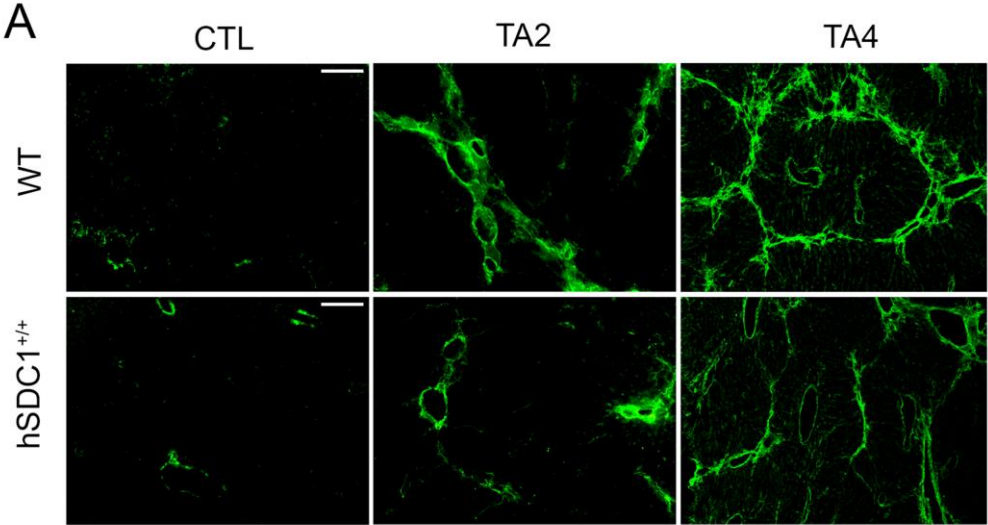
Figure 3.
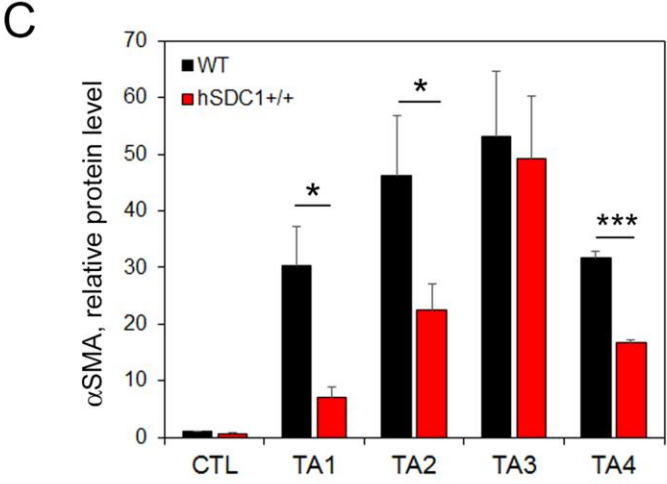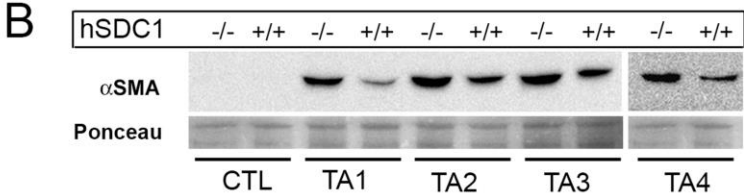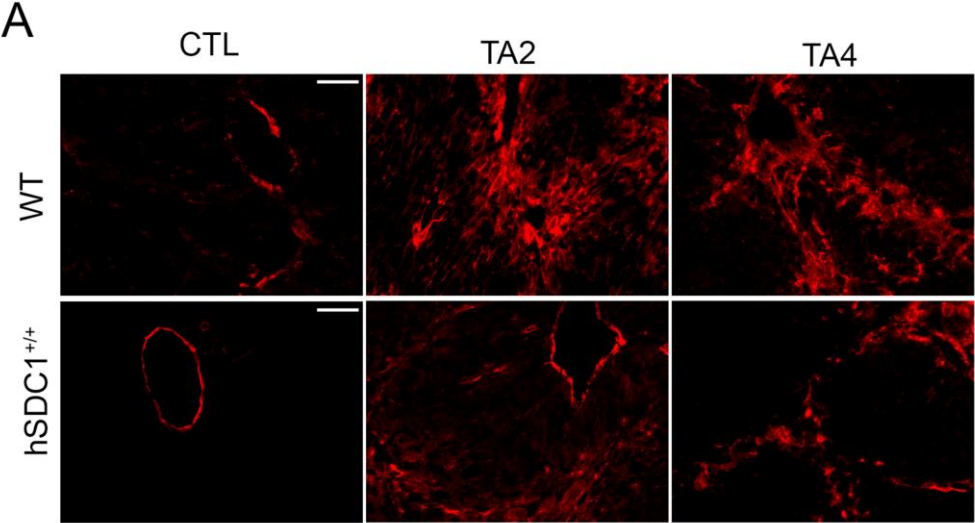
Figure 4.
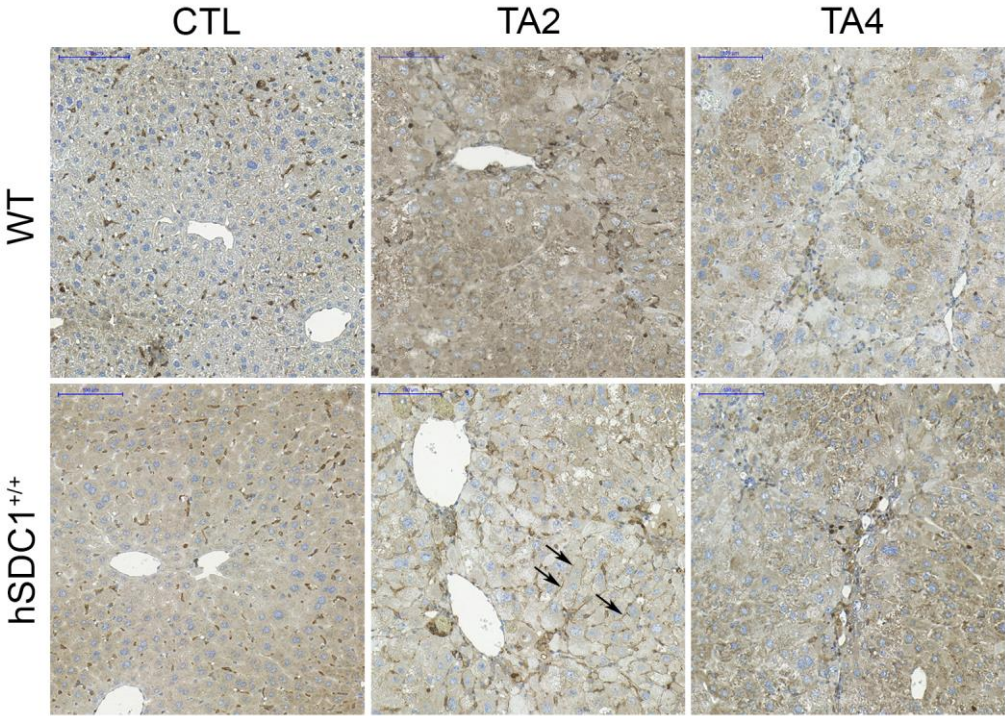
Figure 5.
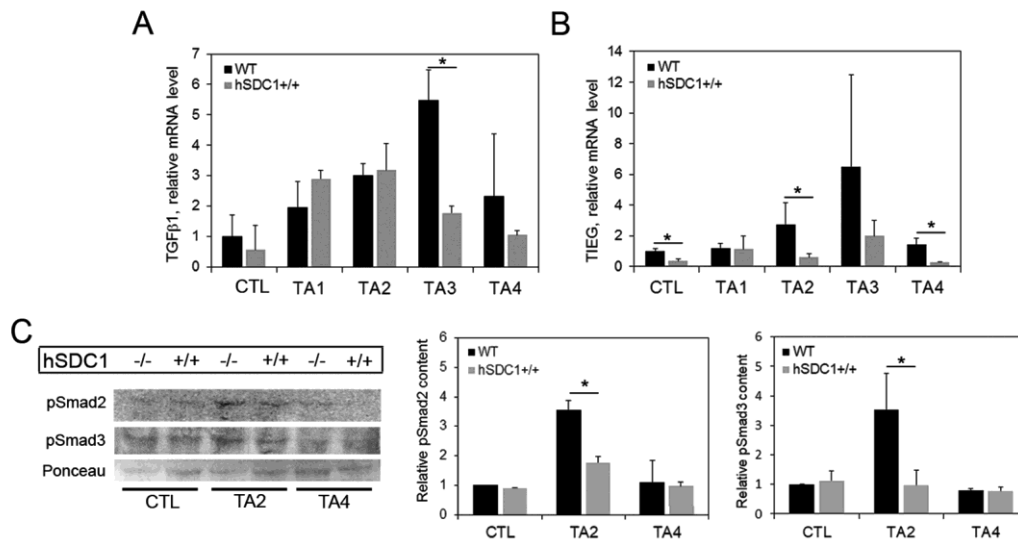
Figure 6.

Figure 7.

Figure 8.

A

CTL   TA2   TA4

WT

hSDC1+/+

human syndecan-1

B

WT

hSDC1+/+

heparan sulfate

C

D

Figure 9.

Figure S1.

A

mAlb/hSynd1
8268 bps

Sall 32
Ecil 7500
EcoRI 1332
Ecil 6670
Mus. Alb. prom
Ecil 5842
Ecil 5696
hSynd1 F 306
Hu. Syndecan1
hSynd1 R655
HindIII 2464
Sall 5250
PolyA
EcoRI 3388
Ecil 4381
Ecil 4370
Ecil 4360
Ecil 3685

B

PolyA RNA   DNA control
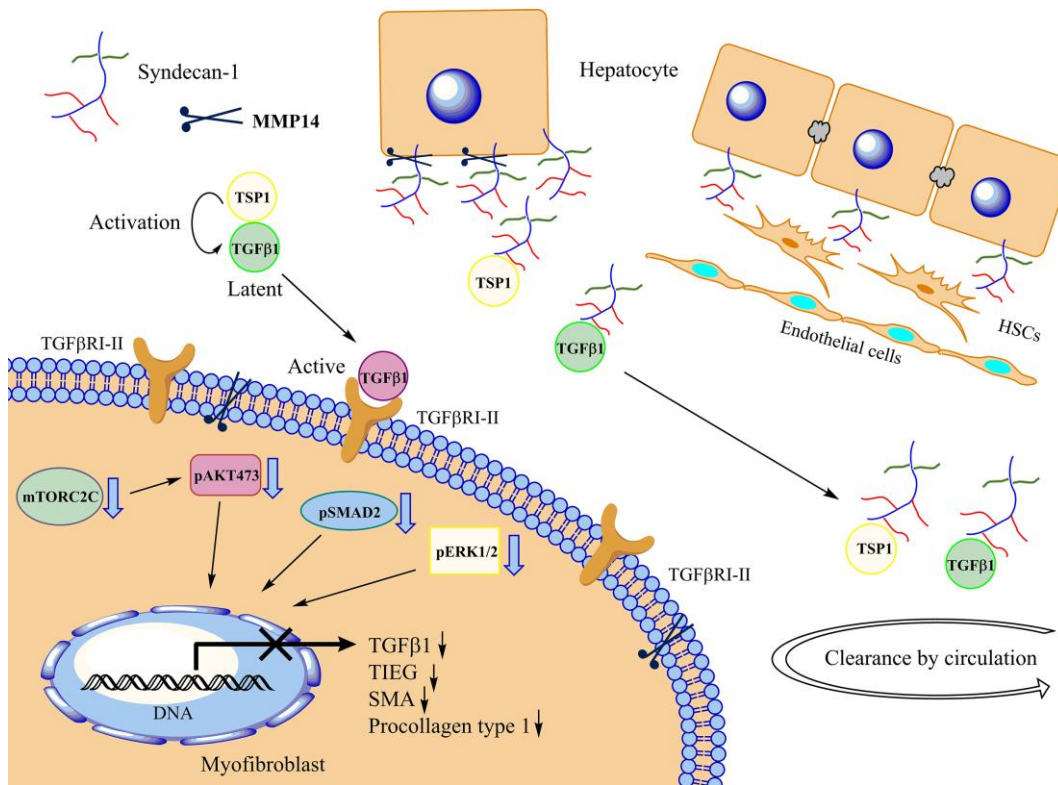#2   #15   #18   #2   #15   #18   NTC

C
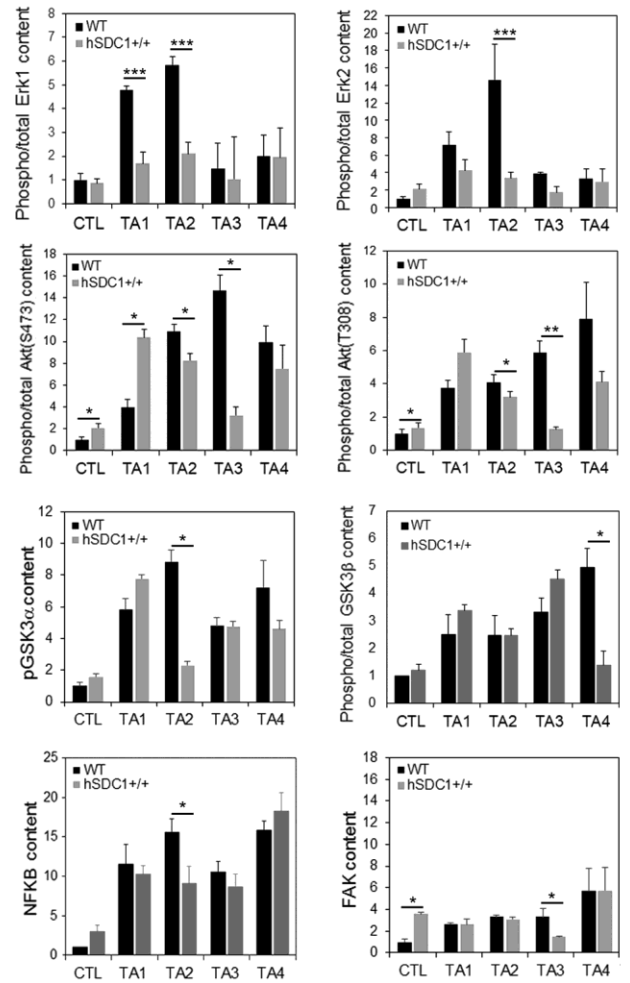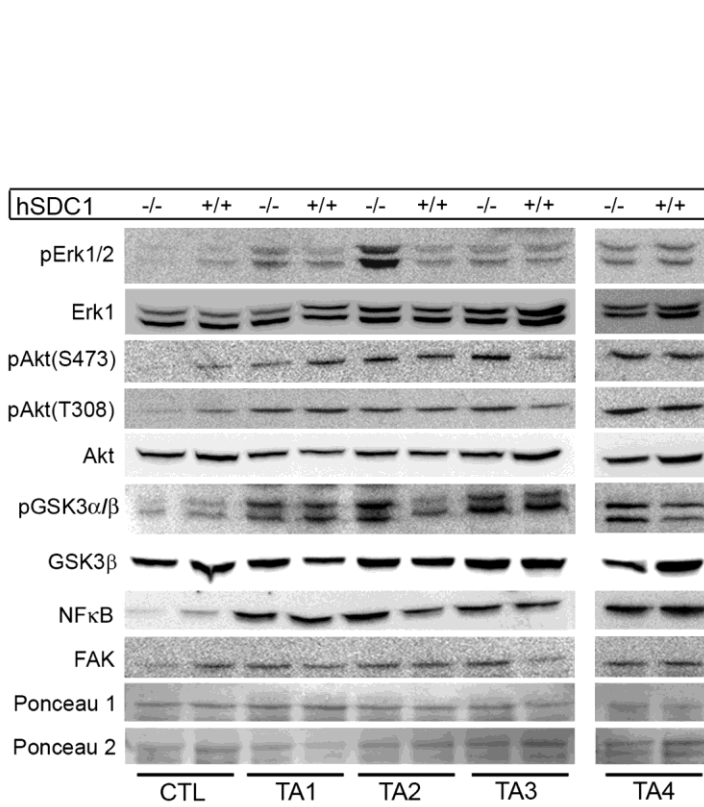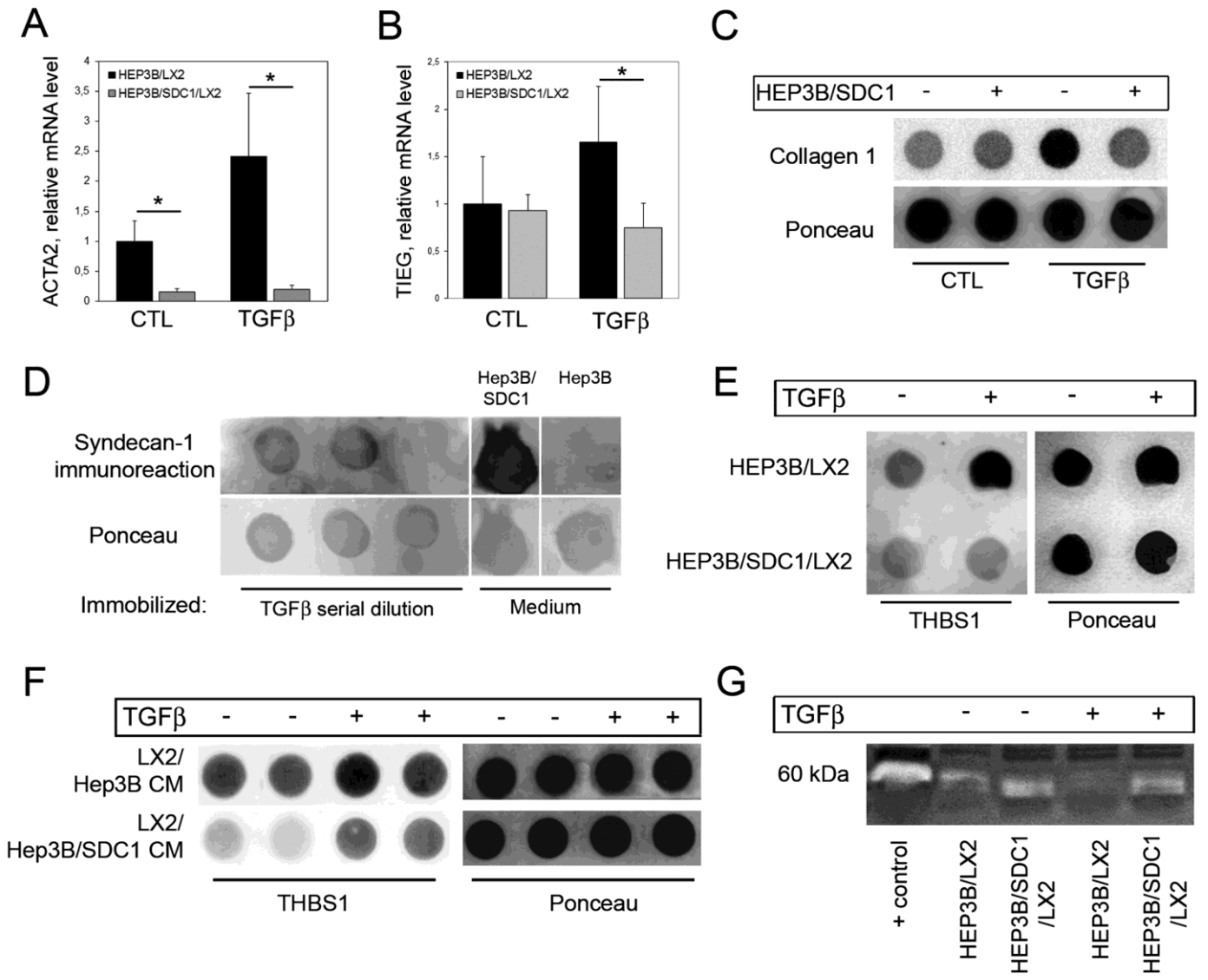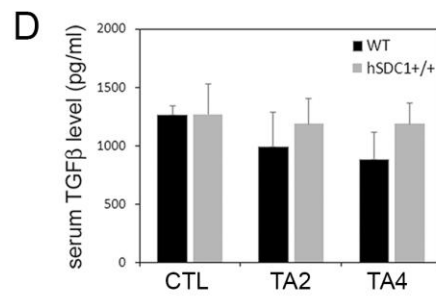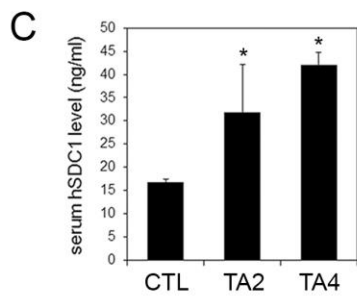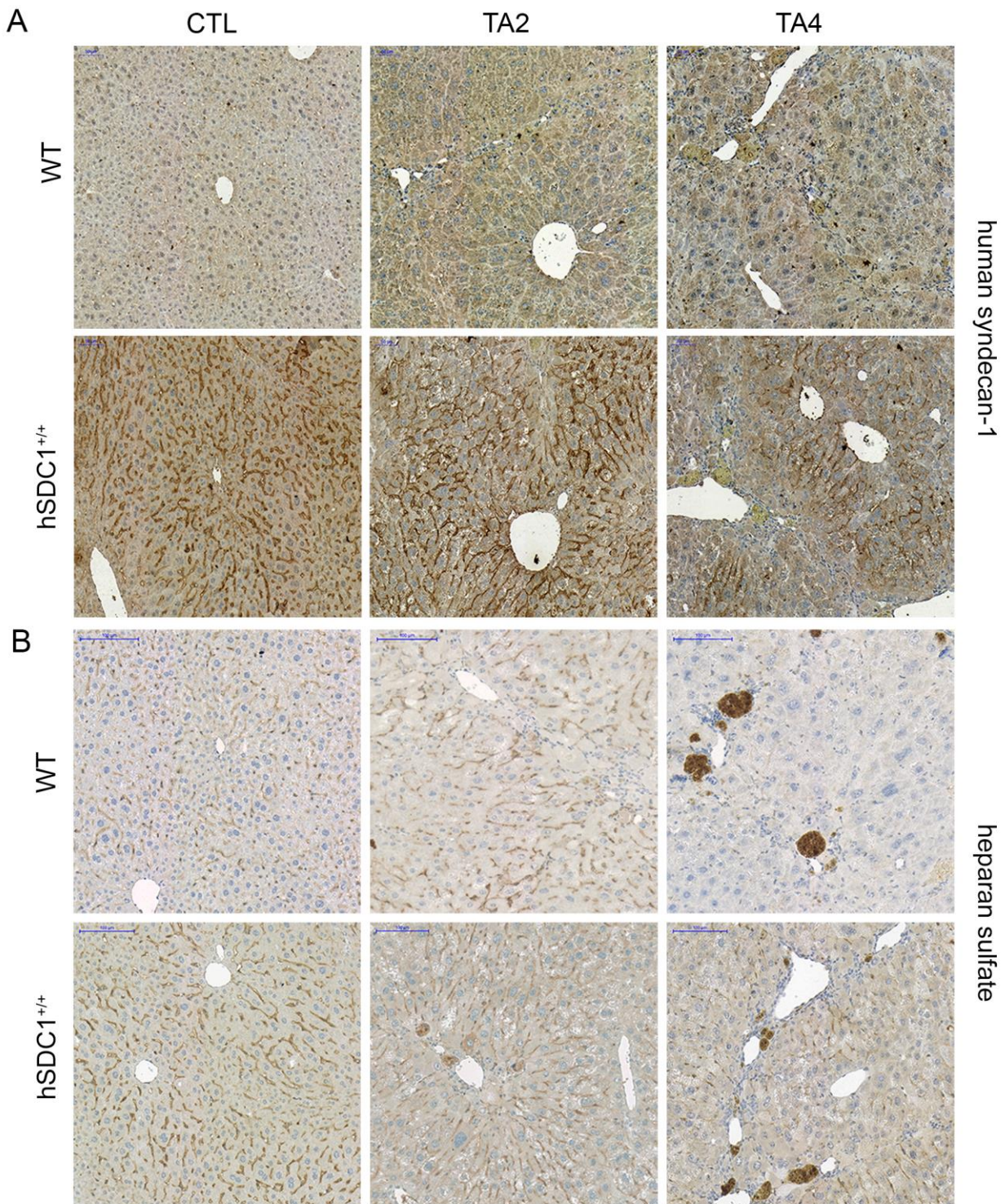
Wild type   hSDC1⁺/⁺
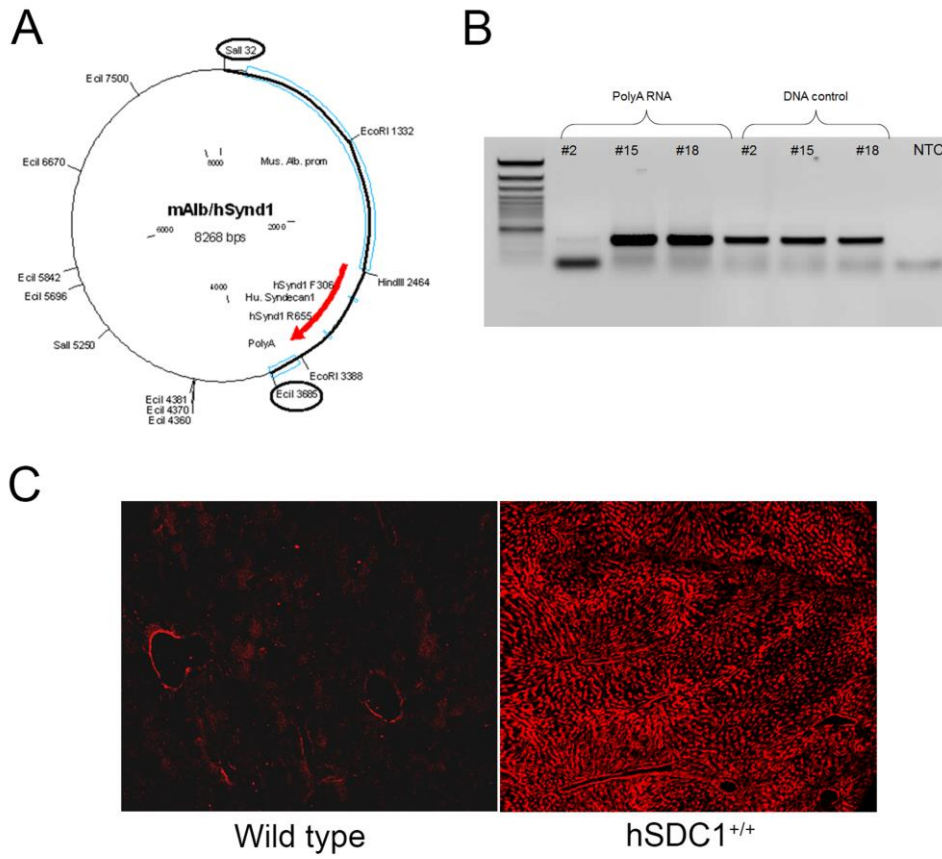
Figure S2.
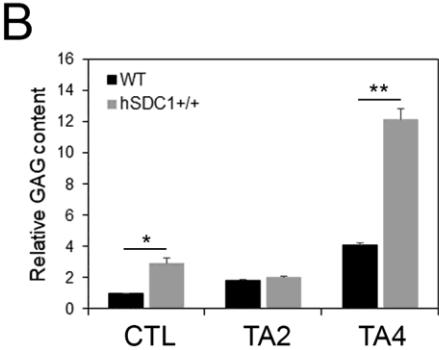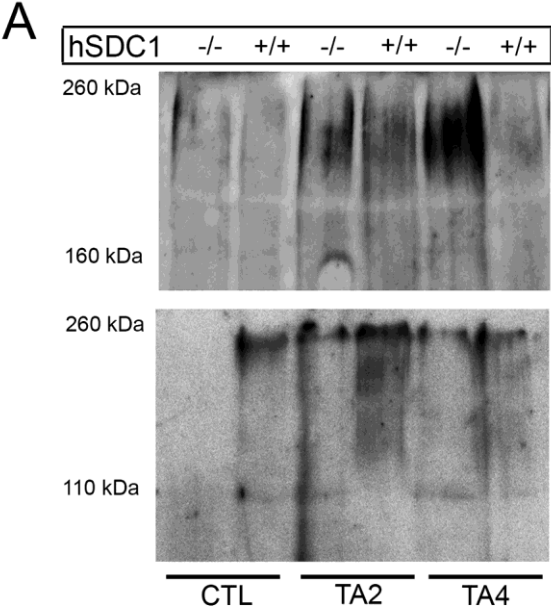
Supplementary Table 1. List of antibodies

Name of antibody	Cat. No.	Provider	Application	Dilution
Alpha-actin (smooth muscle)	1184-1	Epitomics	Western	1:1000
Alpha-actin (smooth muscle)	1184-1	Epitomics	IHC	1:100
phospho-Akt (Thr308)	2965	Cell Signaling	Western	1:1000
phospho-Akt (Ser473)	4058	Cell Signaling	Western	1:1000
Anti-Collagen 1	ab34710	AbCam	Dot-blot	1:1000
Anti-Collagen type I	234167	Calbiochem	IHC	1:100
FAK	3285	Cell Signaling	Western	1:1000
phospho-GSK-3 α/β (Ser21/9)	9331	Cell Signaling	Western	1:1000
NFkB (D14E12)	8242	Cell Signaling	Western	1:1000
phospho-p44/42 MAPK	4370	Cell Signaling	Western	1:1000
phospho-Smad2 (Ser465/467) Clone 1385D	12747	Cell Signaling	Western	1:1000
phospho-Smad3 (Ser423/425) Clone C25A9	12747	Cell Signaling	Western	1:500
Anti-Syndecan-1	MABT-516	Merck	Dot-blot	1:1000
Anti-Syndecan-1	MABT-516	Merck	IHC	1:500
Heparan Sulfate (10E4 epitope)	370255-S	Seikagaku, Amsbio	Western	1:500
Thrombospondin 1	sc-12312	Santa Cruz	Western	1:500
MMP-14	EP1264Y	AbCam	IHC-P	1:400
GSK-3β (clone 27C10)	9315	Cell Signaling	Western	1:1000
Akt	4691s	Cell Signaling	Western	1:1000
Erk1/2	4695s	Cell Signaling	Western	1:1000
Human Syndecan-1 ECM	AF2780	R&D	IHC-p	10 µg/ml
Mouse Syndecan-1 ECM	AF3190	R&D	Western	1:1000
Syndecan-1	3643R-100	BioVision	Western	1.500
Heparan-Sulfate (10E4)	370255-S	Amsbio	IHC-p	1:75
Secondary antibodies				
Donkey anti-Rabbit IgG (H+L), Alexa Fluor 555	A-31572	Molecular Probes, Invitrogen	IHC, ICC	1:200
Donkey anti-Goat IgG (H+L), Alexa Fluor 488	A-11055	Molecular Probes	IHC, ICC	1:200
Goat anti-Rabbit Immunoglobulins/HRP	P0448	Dako	Western, Dot-blot	1:2000
Rabbit anti-Goat Immunglobulins/HRP	P0449	Dako	IHC-p	1:200
Rabbit anti-Goat Immunoglobulins/HRP	P0449	Dako	Western	1:2000

Supplementary Table 2. List of gene expression assays.

Mouse	Assay ID
Col1A1	Mm00801666_g1
TIEG	Mm00449812_m1
TGFβ1	Mm01178820_m1
β-actin	Mm00607939_s1
Human	**Assay ID**
αSMA	Hs.PT.56a.21389192
TIEG	Hs.PT.58.424187.gs
GAPDH	Hs.PT.39a.22214836